1991RMxAA..22..255A

Rev. Mexicana Astron. Astrof., **22**, 255-263 (1991)

AN IMPROVED MODEL OF THE GALACTIC MASS DISTRIBUTION FOR ORBIT COMPUTATIONS

Christine Allen and Alfredo Santillán

Instituto de Astronomía and
Dirección General de Servicios de Cómputo Académico
Universidad Nacional Autónoma de México

Received 1991 April 16

RESUMEN

Se presenta un modelo realista, pero sencillo y analítico para la distribución de masa de la Galaxia, el cual constituye una versión mejorada del potencial propuesto por Allen y Martos (1986, Paper 1). El nuevo potencial es completamente analítico; la densidad puede obtenerse de él en forma cerrada y es positiva en todo el espacio. Se mantiene la gran simplicidad matemática, así como la buena representación de la curva de rotación observada y de la fuerza perpendicular al plano. El nuevo potencial consiste de un bulbo central y un disco, ambos de la forma propuesta por Miyamoto y Nagai (1975), y de un halo masivo similar al de nuestro trabajo anterior. La masa total del modelo es de 9.00×10^{11} masas solares, la velocidad de escape para objetos en el entorno solar, de 535.7 km s^{-1}. Los valores que se obtienen para las constantes de la rotación galáctica son A = 12.95 km s^{-1} kpc^{-1} y B = -12.93 km s^{-1} kpc^{-1}, en buena concordancia con los datos actuales. A diferencia de otros modelos recientes para la galaxia, el potencial que proponemos es extremadamente simple, completamente analítico, continuo y con derivadas continuas en todo sitio. La utilidad del modelo para el cálculo numérico eficiente y preciso de órbitas galácticas se demuestra recalculando las órbitas de algunas estrellas cercanas de alta velocidad. Las características orbitales de estas estrellas resultan ser muy similares a las obtenidas con el modelo anterior.

ABSTRACT

A realistic, yet very simple and analytical model for the galactic mass distribution is presented, which improves upon a similar model proposed in Allen and Martos (1986, Paper 1). The new potential is completely analytical; the density can be obtained from it in closed form and it is positive everywhere. Extreme mathematical simplicity is retained, as well as a good representation of the observed values of both the rotation curve and the perpendicular force. The new model consists of a spherical central bulge and a disk, both of the Miyamoto - Nagai (1975) form, plus a massive, spherical, halo similar to that of Paper 1. The total mass of the model is 9.00×10^{11} solar masses. The model escape velocity for objects in the solar vicinity is 535.7 km s^{-1}. The values obtained for the galactic rotation constants are A = 12.95 km s^{-1} kpc^{-1} and B = -12.93 km s^{-1} kpc^{-1}; they are in good agreement with recent observational data. In contrast to other models for our galaxy, the proposed potential function is extremely simple, fully analytical, continuous, and with continuous derivatives everywhere. The suitability of this potential for efficient and accurate numerical orbit computations is demonstrated by recalculating the orbits of several nearby, high velocity stars. The orbital characteristics of these stars are found to be quite similar to those obtained with the previous model.

Key words: **GALAXY-STRUCTURE – STARS-DYNAMICS**

I. INTRODUCTION

Dynamical mass models of the galaxy utilize as input the available observational data on the radial and perpendicular forces. The galactic rotation curve contains information about the radial force field on the plane at various radial distances; unfortunately, there is no way to obtain similar information about the run of the perpendicular force over a wide range of radial values; our

© Universidad Nacional Autónoma de México • Provided by the NASA Astrophysics Data System

1991RMxAA..22..255A

knowledge is restricted to determinations at the solar circle, and reaching only to about 500 pc in z. However incomplete, these data comprise the most direct sampling of the galactic gravitational field available today. In order to build galactic mass models, this information usually has to be supplemented by other, less direct data, and by analogies with external galaxies. The scarcity of observational material directly related to the galactic potential field makes it desirable to keep theoretical models as simple as possible.

A few years ago we developed a simple galactic mass model based primarily on the rotation curve and on the run of the perpendicular force (Allen and Martos 1986). The model consisted of a central mass point, a modified Ollongren disk and a massive spherical halo, and it proved to be quite useful for the purpose for which it was constructed, namely numerical orbit integrations (Allen and Martos 1988; Allen 1990; Allen, Schuster and Poveda 1991). However, the model had some unsatisfactory features; one was the artificiality of the central mass point adopted; another was the unphysical behaviour of the Ollongren disk at certain intermediate values of R and z. Ollongren (1962) himself noticed this anomaly, which manifests itself in the shoulder that appears in the z-force at values of z between about 0.6 and 1.0 kpc. Though in a much attenuated form due to the smaller relative contribution of the disk, the shoulder is also present in our model. In fact, if one computes via Poisson's equation the density in this region, it turns out to be negative. Ollongren investigated the effect of this local force irregularity on the computed orbits, and found it to be negligible, a fact that we, too, confirmed in the course of many integrations. Although unimportant for the computed orbits, this feature of the model is still disturbing.

A new galactic mass (or potential) model is proposed, which avoids the difficulties just mentioned and takes into account the recent values for R_o and $V(R_o)$ recommended by the IAU (Kerr and Lynden-Bell 1986), as well as new proper motion results (Hanson 1987) that largely eliminate the need for a falling rotation curve at the solar vicinity. The new model is based on the potential-density pairs proposed by Miyamoto and Nagai (1975). Our aim has been to retain the mathematical simplicity of the first model, and to keep the number of components used to the absolute minimum necessary to obtain a good representation of the rotation curve and of the perpendicular force.

The present model consists of only three components: a spherical central mass distribution, a disk, and a massive halo. Both the central component and the disk are of the Miyamoto-Nagai form. The halo is very similar to that of Paper 1.

In a recent paper, Carlberg and Innanen (1987) use a model based on the Miyamoto-Nagai potential to determine the circular velocity at the Sun's circle. Our approach differs from theirs in that they achieve only a rough fit to the rotation curve, and do not attempt any fit at all to the perpendicular force. Even so, they find it necessary to introduce a spherical bulge component in addition to the central mass distribution, so theirs is a four-component model. As we shall show, an excellent fit to both the rotation curve and the perpendicular force can be obtained with only three components. Moreover, Carlberg and Innanen incorporate into their model the value they obtain for the circular velocity at the Sun's circle, namely 235 km s^{-1}, although this value is somewhat different from the recommended IAU value, namely 220 km s^{-1}; furthermore, they assume a local mass density of 0.19 $M_\odot$ pc^{-3}, a value perhaps too high in view of recent, though controversial, results (Kuijken and Gilmore 1989). For these reasons, the model proposed by Carlberg and Innanen is not entirely satisfactory.

The present paper is organized as follows: in §II, the adopted observational constants and constraints are discussed; further, the mass model is presented and compared with available observational data. §III contains the results of numerically integrating the galactic orbits of some stars of particular interest. In the final section a brief summary of our results and conclusions is given.

II. OBSERVATIONAL CONSTRAINTS AND MODEL PARAMETERS

a) *Adopted Observational Constraints*

Following recent recommendations of the IAU (Kerr and Lynden-Bell 1986), we adopt R_o = 8.5 kpc as the Sun's galactocentric distance, and $V_o(R_o)$ = 220 km s^{-1} as the circular velocity at the Sun's position. Further, we assume that the massive dark halo of the galaxy extends to a radius of 100 kpc.

As in Paper 1, we have attempted to achieve a good fit of our model with the observational parameters most reliably established, namely, the galactic rotation curve and the perpendicular force at the solar circle. Of course, this information is not sufficient to fully specify the galactic potential. Additional factors that were taken into account were physical plausibility of the model, as well as similarity of the resulting global rotation curve to that of external galaxies of morphological type and total luminosity similar to our own (Rubin, Ford and Thonnard 1980; Roberts and Whitehurst 1975; Rubin 1983). We also attempted to achieve compatibility with recent results on the kinematics of nearby stars (Hanson 1987). For the outermost parts of the model we opted for a conservative approach, trying to obtain a flat curve at a moderate

© Universidad Nacional Autónoma de México • Provided by the NASA Astrophysics Data System

1991RMxAA..22..255A

velocity of about 200 km s^{-1} . This approach will give a moderate value for the total mass of the model galaxy (less than 10^{12} $M_\odot$), implying a local escape velocity of less than about 550 km s^{-1} .

Essentially the same values as in Paper 1 were taken (see the references listed there) for the galactic rotation curve inside the solar circle except that they were scaled, when necessary, to the new adopted values for R_o and for the circular velocity at R_o. For the points just outside the solar circle we use, as in Paper 1, the normal points advocated by Haud (1984), scaled to the galactic constants here adopted. However, since recent results on the proper motions of nearby stars no longer indicate $|B| < |A|$, i.e., a falling rotation curve just outside the solar circle (Hanson 1987), a major discrepancy between optical and radio-astronomical data has been removed, and we can now settle for a nearly flat rotation curve in this region, very gently falling off beyond 10 kpc, and becoming flat beyond about 40 kpc at a value close to 200 km s^{-1} . For the region just outside the solar circle, we have also taken into account recent results obtained by Fich, Blitz and Stark (1989), as shown in Figure 3. As previously stated, we adopt for the outermost parts of the model a flat rotation curve with a velocity of just under 200 km s^{-1} , since this will give the smallest values for the total mass of the Galaxy.

TABLE 1

ADOPTED OBSERVATIONAL CONSTRAINTS AND MODEL CONSTANTS

Distance Sun - Galactic Center:	$\tilde{\omega}_0$ = 8.5 kpc	
Local circular velocity:	Θ_0 = 220 km s^{-1}	
Local total mass density:	ρ_0 = 0.15 $M_\odot$ pc^{-3}	
Rotation curve:	$\tilde{\omega}$ (kpc)	Θ (km s^{-1})
	0.43	259.8 ± 10
	1.28	226.2 ± 9.7
	2.55	201.5 ± 9.7
	4.25	213.5 ± 7.5
	6.38	224.0 ± 7.8
	10.63	209.0 ± 15
	15.94	223.0 ± 20
	56.63	206.0 ± 40
Central mass constants:	M_1 = 606.0	
	b_1 = 0.3873	
Disk constants:	M_2 = 3690.0	
	a_2 = 5.3178	
	b_2 = 0.2500	
Halo constants:	M_3 = 4615.0	
	a_3 = 12.0	

In recent times, both the perpendicular force and the total mass density in the solar vicinity have been subject to a lively controversy. Studies by Kuijken and Gilmore (1989) seem to indicate a much lower value for the local mass density (0.10 $M_\odot$ pc^{-3}) than previously thought, implying little or no dark matter. These results are in contradiction to nearly 30 years of astronomical work, and have caused a great deal of discussion and dissent. As an example, in a recent paper Bahcall (1991) casts doubt on the Kuijken and Gilmore results, and obtains values for the local density of 0.26 $M_\odot$ pc^{-3} or even higher. Thus, the matter is far from settled. Following our conservative approach here too, we adopt a value for the total mass density in the solar vicinity of 0.15 $M_\odot$ pc^{-3}, which seems a reasonable compromise between recent results and previously obtained values of about 0.19 $M_\odot$ pc^{-3} (Bahcall 1984). Should a significantly different value for the local mass density become widely accepted, the galactic mass model we propose would have to be suitably adjusted; the adjustment can be accomplished in a fairly straightforward way, since it involves only recalculating the constants a_2 and b_2 (see §IIc, below).

Table 1 summarizes the assumed observational constraints and the constants used for the fit of our mass model.

b) *Central Mass Distribution*

In Paper 1 the central mass distribution of the galaxy was assumed to be sufficiently well represented by a mass point; this rather artificial approximation was taken because the great majority of stellar orbits of astronomical significance do not penetrate the central kiloparsec or so of the galaxy. However, subsequent work has shown that a significant fraction of those orbits that do attain pericentric distances of less than about 1 kpc are chaotic (Allen, Schuster and Poveda 1991). This behavior is conjectured to be a consequence of the dominance of the spherically symmetric mass distribution in the central region (Aarseth 1966; Martinet 1974; Carlberg and Innanen 1987), but the exact role that such a distribution as opposed to a mass point may play is unknown. Now, the existence of a significant number of chaotic orbits will tend to smear out any correlations of orbital characteristics with age or metallicity (Allen, Schuster and Poveda 1991). Therefore, it is interesting to investigate the effects of using a less artificial, though still spherically symmetric, potential for the central region. For these reasons, we adopt in the present paper a spherically symmetric potential of the form (Miyamoto and Nagai 1975)

$$\phi_1(\varpi,z) = -\frac{M_1}{(\varpi^2+z^2+b_1^2)^{1/2}} \,. \qquad (1)$$

© Universidad Nacional Autónoma de México • Provided by the NASA Astrophysics Data System

1991RMxAA..22..255A

The corresponding expression for the density is

$$\rho_1(\varpi,z)=\frac{3b_1^2M_1}{4\pi(\varpi^2+z^2+b_1^2)^{5/2}}. \quad (2)$$

It should be noticed that equation 1 corresponds, in fact, to the original Plummer model (Plummer 1911). If R is given in kpc and M_1 in galactic mass units (1 galactic mass unit = 2.32×10^7 $M_\odot$), then $G = 1$, and units for ϕ are 100 km^2 s^{-2}. We will use cylindric galactic coordinates $\tilde{\omega}$, z, θ, and their corresponding velocities Π, Z, Θ throughout. Then, $R^2 = \tilde{\omega}^2 + z^2$. The constant M_1 in (1) is related to the relative importance of the central component, and b_1 is a scale length. Both were determined by successive trials, aiming at a good fit of the total rotation curve of the model galaxy to the observational points adopted. As in Paper 1, it is the innermost points of the rotation curve that mostly determine the parameters of the central mass distribution. The total mass of the central component is 1.41×10^{10} $M_\odot$.

The central mass distribution adopted is quite appropriate for orbits that do not approach the innermost kiloparsec of the galaxy. Although it is not intended to represent the detailed and complicated dynamics near the galactic center (at $R < 0.4$ kpc), it should be definitely better than a mass point for very eccentric orbits, where the star spends a short time in the central region (near pericenter) and should allow a more reliable determination of the character of such orbits.

c) *Disk Component*

In the present model, the Ollongren disk of Paper 1 is substituted by a Miyamoto-Nagai disk potential of the form

$$\phi_2(\varpi,z)=-\frac{M_2}{\{\varpi^2+[a_2+(z^2+b_2^2)^{1/2}]^2\}^{1/2}}. \quad (3)$$

The density corresponding to the disk potential is

$$\rho_2(\varpi,z)=\left(\frac{b_2^2M_2}{4\pi}\right)$$

$$\left(\frac{a_2\varpi^2+[a_2+3(z^2+b_2^2)^{1/2}][a_2+(z^2+b_2^2)^{1/2}]^2}{\{\varpi^2+[a_2+(z^2+b_2^2)^{1/2}]^2\}^{5/2}(z^2+b_2^2)^{3/2}}\right). \quad (4)$$

Units for ϕ are again 100 km^2 s^{-2}, if $\tilde{\omega}$ and z are given in kpc. The constant M_2 determines the relative importance of the disk component; a_2 and b_2 are scale lengths. M_2 and $(a_2 + b_2)^2$ were obtained from the fit of the total rotation curve to the adopted observational constraints. Then a_2 and b_2 can obtained separately by inserting the numerical value of the local mass density, here taken as 0.15 $M_\odot$ pc^{-3}. The total mass of the disk is 8.56×10^{10} $M_\odot$.

d) *Halo Component*

In our updated model, the halo potential has a similar form to that of Paper 1, although the numerical values for the constants differ somewhat. The best fit was obtained for a halo potential given by

$$\phi_3(R)=-\left(\frac{M(R)}{R}\right)-\left(\frac{M_3}{1.02a_3}\right)$$

$$\left[-\frac{1.02}{1+(R/a_3)^{1.02}}+\ln\{1+(R/a_3)^{1.02}\}\right]_R^{100}, \quad (5)$$

where

$$M(R)=\frac{M_3(R/a_3)^{2.02}}{1+(R/a_3)^{1.02}}.$$

The form chosen for the halo potential assures that for large values of R, $M(R) \sim R$, as desired.

Units for ϕ are 100 km^2 s^{-2} if R is given in kpc and $M(R)$ in galactic mass units. Equation (5) includes an arbitrary cutoff for the halo at 100 kpc. This cutoff can easily be changed, should a different galactic limiting radius be more desirable.

The density associated to this halo potential is

$$\rho_3(R)=\frac{M_3}{4\pi a_3R^2}(R/a_3)^{1.02}\frac{[2.02+(R/a_3)^{1.02}]}{[1+(R/a_3)^{1.02}]^2}. \quad (6)$$

If R is given in kpc, the resulting units for M are galactic mass units. The total mass of the halo out to 100 kpc is 8.002×10^{11} $M_\odot$. The halo contributes 0.007 $M_\odot$ pc^{-3} to the local mass density. Note that the expression for the force derived from equation (5) is particularly simple, since it involves only the first term. This allows speedy numerical integrations of the orbits. The exponent in equations (5) and (6) was chosen so as to obtain a good fit to the outermost parts of the rotation curve. The point at 57 kpc turned out to be very sensitive to the value of the exponent, effectively preventing the use of mathematically simpler values, like 2.

The total potential is then

© Universidad Nacional Autónoma de México • Provided by the NASA Astrophysics Data System

1991RMxAA..22..255A

$$\phi_T(\varpi,z)=\phi_1(\varpi,z)+\phi_2(\varpi,z)+\phi_3(\varpi,z)\ . \qquad (7)$$

The contributions to the rotation curve arising from the three mass components of the model and the total rotation curve are listed in Table 2. Figure 1 shows the rotation curve of each of the three components, and Figure 2 the total rotation curve together with the observational data adopted. The error bars represent the estimated uncertainties in the data. It can be easily seen that the agreement is excellent. Note that contrary to what Carlberg and Innanen state, it is not necessary to introduce an additional bulge component to prevent the rotation curve from falling below 200 km s^{-1} between 1.5 and 3 kpc. Figure 3 shows a detailed comparison of part of our rotation curve with the data recently obtained by Fich, Blitz and Stark (1989). Specifically, we plot the binned data of their Figure 3, along with their uncertainties. Note that in spite of the binning in 1 kpc intervals, the data remain quite noisy and difficult to fit with any smooth curve. Fich, Blitz and Stark interpret the slight dip observed near R = 10 kpc as a local irregularity associated with the Perseus arm, and state that their derived rotation curve *is flat or at most gently rising to 2* R_0. By the same token, the points lying above the general trend could also be interpreted as due to local irregularities or streaming motions. Figure 3 shows that the newer data are not incompatible with a nearly flat but gently falling rotation curve, such as the one we obtain. In fact, these data are quite similar to the normal points we have adopted for the region just ouside the solar circle (see Figure 2 and Table 1). As stated before, a nearly flat rotation curve in the solar vicinity implies |B| < |A|, in concordance with the proper-motion results of Hanson (1987).

TABLE 2

CONTRIBUTIONS TO THE ROTATION CURVE

$\tilde{\omega}$ (kpc)	Θ (km s^{-1})	Central Mass (km s^{-1})	Disk (km s^{-1})	Halo (km s^{-1})
1	232.39	221.67	45.15	53.15
2	202.80	169.33	84.43	72.99
3	200.89	140.38	114.57	86.73
4	206.69	122.23	135.36	97.25
5	212.60	109.60	148.37	105.70
6	216.70	100.19	155.64	112.70
7	219.00	92.83	158.96	118.63
8	219.91	86.88	159.70	123.73
9	219.91	81.94	158.80	128.17
10	219.32	77.76	156.88	132.08
15	213.81	63.53	142.37	146.31
20	208.93	55.03	128.44	155.33
25	205.57	49.23	117.16	161.58
30	203.28	44.94	108.12	166.17
35	201.70	61.61	100.77	169.69
40	200.56	38.92	94.67	172.47
45	199.73	36.69	89.53	174.73
50	199.10	34.81	85.12	176.59
60	198.24	31.78	77.92	179.50
70	197.70	29.42	72.26	181.65
80	197.34	27.52	67.67	183.32
90	197.08	25.95	63.85	184.64
100	196.90	24.62	60.60	185.72

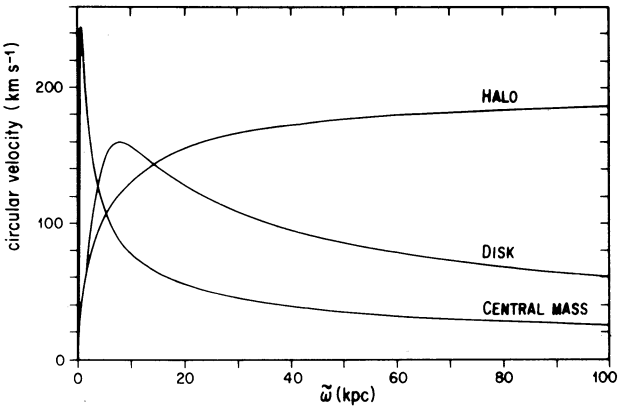

Fig. 1. Contributions of the three mass components to the rotation curve.

Table 3 lists the perpendicular force K_z as a function of z for $\tilde{\omega}$ = 8.5 kpc. Figure 4 compares this force with the data obtained by Oort (1960) for two values of the local density, 0.18 and 0.15 $M_\odot$ pc^{-3}, by Bahcall (1984) for his preferred proportional model (with a local density of 0.18 $M_\odot$ pc^{-3}), and by Kuijken and Gilmore (1989) for a density of 0.10 $M_\odot$ pc^{-3}. In spite of the rather large uncertainties of the observational determinations the perpendicular force resulting from our model can be considered to be in excellent agreement with the higher density data. The integrated surface mass density between z = −1.1 kpc and z = + 1.1 kpc can be shown to be 140.65 $M_\odot$ pc^{-2} for our model. This value is a factor of two larger than that obtained by Kuijken and Gilmore (1991), another manifestation of the significantly lower densities near the Sun found by these authors.

Figure 5 shows the run of K_z with z for different values of $\tilde{\omega}$. In the region near $\tilde{\omega}$ = 8.5 kpc K_z reaches a shallow maximum with a value of $-K_z = 9.9 \times 10^{-9}$ cm s^{-2} at z = 3.3 kpc, which is not far from the observational value $-K_z = 9.1 \times 10^{-9}$ cm s^{-2} (Caldwell and Ostriker 1981).

Figure 6 shows equipotential surfaces, Figure 7 contours of equal density. The distribution of matter appears quite plausible. Both equipotentials and isopleths are smooth everywhere. As in Paper 1, all plane circular orbits in our potential are stable,

© Universidad Nacional Autónoma de México • Provided by the NASA Astrophysics Data System

1991RMxAA..22..255A

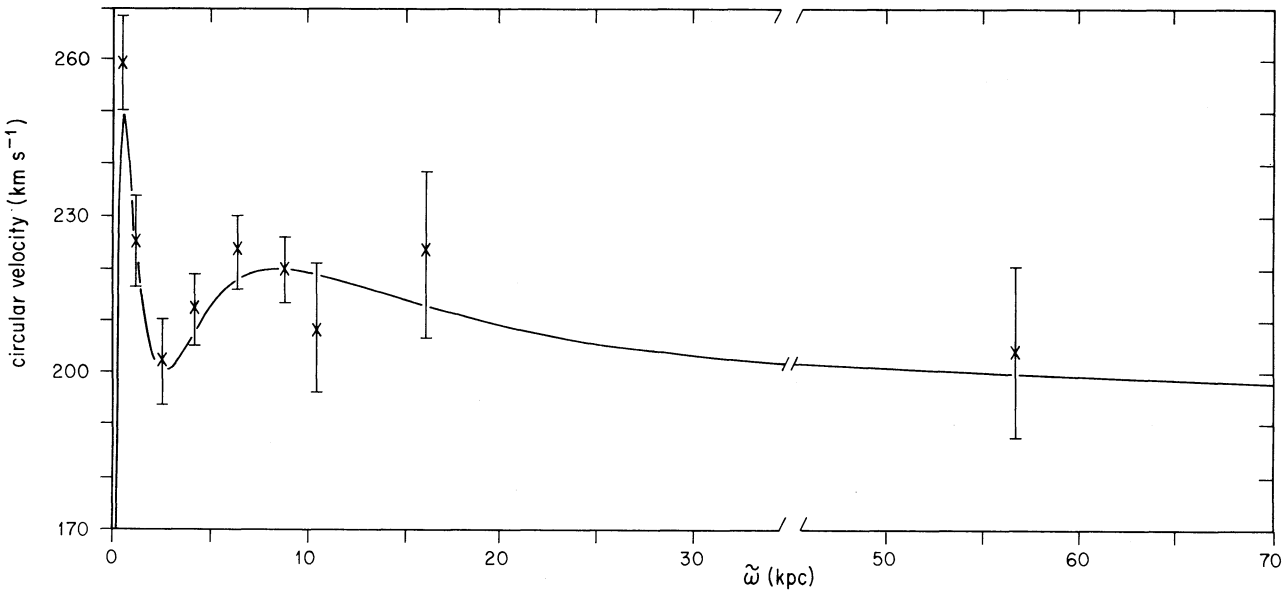

Fig. 2. Total rotation curve resulting from the mass model. The error bars are the estimated uncertainties in the observational data.

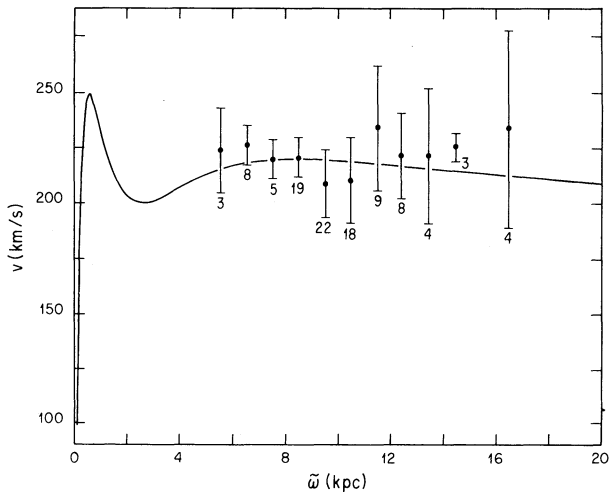

Fig. 3. Detailed comparison of the rotation curve resulting from the present model with recent observational data. We show the CO data obtained by Fich, Blitz and Stark (1989) taken from their Figure 3, along with their estimated uncertainties. To reduce the noise, the data were binned in 1 kpc intervals; the numbers shown correspond to the number of objects in each bin. Note that beyond the solar circle the bins containing the largest numbers of objects tend to fall below the flat curve, whereas the bins containing fewer objects give higher values for the rotational speed.

since h, the orbital angular momentum, increases with $\tilde{\omega}$ everywhere.

Table 4 lists some local parameters computed from our mass model. The values we obtain for Oort's constants are A = 12.95 km s^{-1} kpc^{-1} and B = −12.93 km s^{-1} kpc^{-1}, well within the range of currently accepted observational values (Kerr and Lynden-Bell 1986, and references therein).

The total mass of our model is 9.00 × 10^{11} $M_\odot$, assuming the halo is truncated at 100 kpc. This value compares well with recent determinations of the mass of the Milky Way. Zaritsky *et al.* (1989), for example, obtain values for the galactic mass of 9.3 × 10^{11} $M_\odot$ to 12.5 × 10^{11} $M_\odot$, depending on whether they assume radial or isotropic orbits for remote galactic satellites.

TABLE 3

RUN OF K_z VERSUS z FOR $\tilde{\omega}$ = 8.5 kpc

z (pc)	$-K_z$ (10^{-9} cm s^{-2})	z (pc)	$-K_z$ (10^{-9} cm s^{-2})
100	2.46	1300	7.52
200	4.17	1400	7.62
300	5.19	1500	7.71
400	5.81	2000	8.11
500	6.21	2500	8.42
600	6.50	3000	8.66
700	6.72	3500	8.84
800	6.90	4000	8.96
900	7.05	4500	9.03
1000	7.19	5000	9.06
1100	7.31	5500	9.05
1200	7.42	6000	9.01

© Universidad Nacional Autónoma de México • Provided by the NASA Astrophysics Data System

1991RMxAA..22..255A

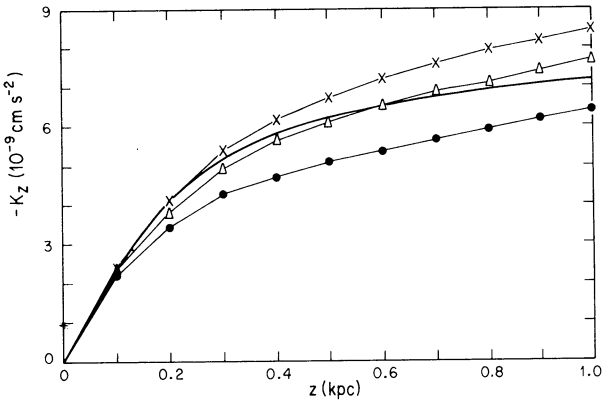

Fig. 4. The perpendicular force K_z as a function of z (solid line). The points shown are the data of Oort (1960) for two values of the local density, $\rho = 0.15$ $M_\odot$ pc^{-3} (dots) and $\rho = 0.15$ $M_\odot$ pc^{-3} (diamonds). Also shown are the values obtained by Bahcall (1984) for his proportionate model with a massive halo (crosses).

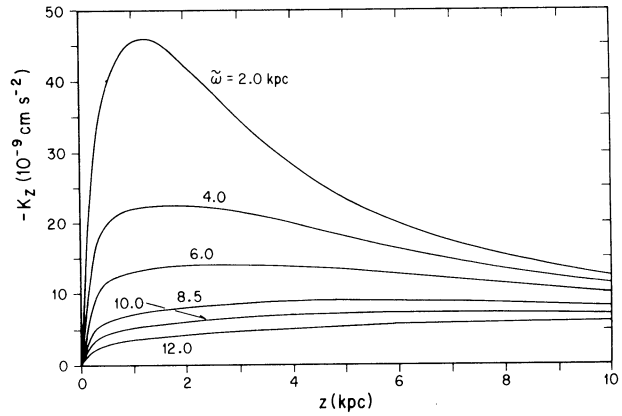

Fig. 5. Run of K_z as a function of z for different values of $\tilde{\omega}$.

TABLE 4

LOCAL PARAMETERS COMPUTED FROM THE MODEL

Rotation constant	A = 12.95 km s^{-1} kpc^{-1}
Rotation constant	B = −12.93 km s^{-1} kpc^{-1}
Period of revolution of local centroid	P = 2.37 × 10^8 y
Angular Velocity of local centroid	$\dot{\theta}_0$ = 25.88 km s^{-1} kpc
Local slope of Θ_0	$[\frac{d\Theta}{d\tilde{\omega}}]_{\tilde{\omega}_0}$ = −0.02 km s^{-1} kpc
Escape velocity	v_e = 535.7 km s^{-1}
Density gradient	$\tilde{\omega}_0 \frac{d}{d\tilde{\omega}}$ (log ρ) = −1.42

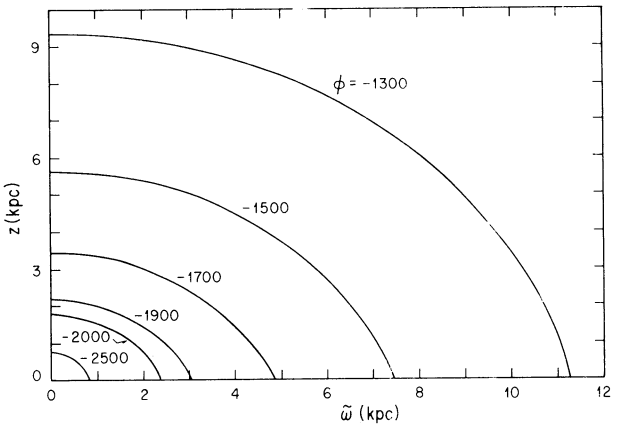

Fig. 6. Some equipotential surfaces resulting from the mass model, shown in the plane $\tilde{\omega}$, z.

TABLE 5

ESCAPE VELOCITY AS A FUNCTION OF $\tilde{\omega}$

$\tilde{\omega}$ (kpc)	v_e (km s^{-1})	$\tilde{\omega}$ (kpc)	v_e (km s^{-1})
1	691.4	20	455.5
2	642.9	25	433.9
3	616.9	30	416.0
4	597.3	35	400.5
5	580.7	40	386.8
6	566.0	45	374.4
7	552.9	50	363.0
8	541.2	60	342.6
8.5	535.7	70	324.5
9	530.5	80	308.1
10	520.8	90	292.8
15	482.8	100	278.5

The model escape velocity in the solar vicinity is v_e = 535.7 km s^{-1} . Currently accepted observational determinations for v_e span the range from $v_e = (640 \pm 96)$ km s^{-1} (Caldwell and Ostriker 1981) to $v_e > 500$ km s^{-1} (Carney, Latham and Laird 1988), 450 km s^{-1} < v_e < 650 km s^{-1} (Leonard and Tremaine 1990), or $v_e > 475$ km s^{-1} (Cudworth 1990). Table 5 lists the model escape velocity for different values of $\tilde{\omega}$.

III. SOME ILLUSTRATIVE ORBITS

To test the present model and to compare its results with those obtained with the model of Paper 1, the galactic orbits of 10 nearby high-velocity stars selected from van de Kamp's (1971) list of stars nearer than 5.2 pc were integrated anew. Also recomputed was the orbit of the interesting binary LDS 519 (Allen, Martos and Poveda 1987, Paper 2).

© Universidad Nacional Autónoma de México • Provided by the NASA Astrophysics Data System

1991RMxAA..22..255A

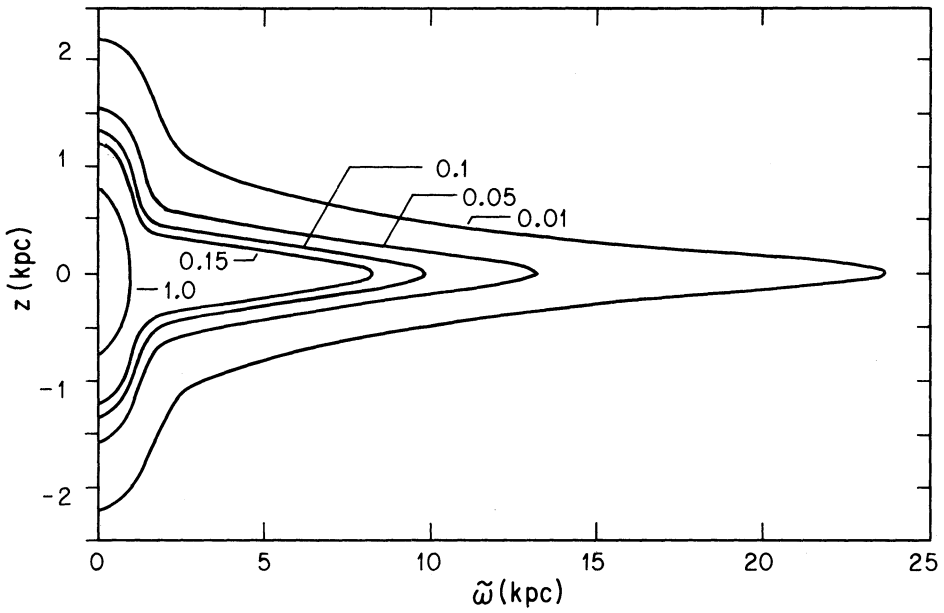

Fig. 7. Contours of equal density resulting from the mass model, shown on the plane $\tilde{\omega}$, z.

The orbits of the stars were numerically integrated backwards in time for 1.6×10^{10} years, an estimated average age for the old nearby stars. The total energy and the z-component of the angular momentum of the star were very well conserved, typically showing cumulative errors of, respectively, $\Delta E/E < 10^{-8}$ and $\Delta h/h < 10^{-9}$ at the end of the run. The computing time for the orbits was found to be on average 1.42 times shorter than with our previous model. Both the greater accuracy and the faster computation speed are consequences of the extreme mathematical simplicity of the present model. These runs demonstrate that the new model is even better suited for direct numerical integrations of galactic orbits.

Table 6 lists "initial conditions" for the selected stars, derived from their observed parameters as listed in Papers 1 or 2. Table 7 contains the main characteristics of the galactic orbits. It is interesting to compare the present results with the corresponding values from Papers 1 or 2. Qualitatively, the orbits are practically indistinguishable (hence we do not show the meridional orbits or surfaces of section). The exceptions are Gliese 166 and 699, which in the new model move in box instead of shell orbits, and Gliese 191, formerly a box and now a shell. These discrepancies are hardly surprising, since the orbital structure of the new model is, in principle, quite different. Quantitatively, the orbital parameters are very similar for all stars, as can be ascertained by comparing Table 7 with the corresponding tables in Papers 1 and 2. For the comparison, it should be borne in mind that different galactic parameters are being used. Even so, the differences are usually smaller than 10%. The greatest discrepancies are found in the case of the weakly bound wide binary LDS 519, particularly in its apocentric distance. These results are reassuring, because they show that the great majority of the computed orbits do not depend sensitively on the details of the adopted galactic mass model, at least as long as the global parameters of the model remain similar.

TABLE 6

INITIAL CONDITIONS FOR NEARBY HIGH-VELOCITY STARS

Star	$\tilde{\omega}$	z	Π	Z	Θ
	(kpc)			(km s^{-1})	
GL1	8.499	−0.004	+ 68.2	− 29.4	+131.8
GL166	8.504	−0.003	−103.7	− 33.8	+219.4
GL191	8.501	−0.002	− 28.2	− 46.4	− 57.1
GL411	8.501	0.002	− 54.7	− 67.6	+178.1
GL445	8.502	0.003	− 79.9	− 71.4	+171.1
GL699	8.498	0.000	+129.4	+ 24.6	+236.5
GL820	8.499	0.000	+ 81.4	− 2.2	+177.5
GL845	8.498	−0.003	+ 68.4	+ 9.8	+193.0
GL887	8.499	−0.003	+ 92.7	− 50.9	+216.3
GL905	8.501	−0.001	− 42.5	+ 7.3	+153.5
LDS519A	8.474	0.019	−313.6	−98.4	−340.6
LDS519B	8.474	0.019	−321.8	− 93.1	−342.4

© Universidad Nacional Autónoma de México • Provided by the NASA Astrophysics Data System

1991RMxAA..22..255A

TABLE 7

PRINCIPAL CHARACTERISTICS OF GALACTIC ORBITS OF NEARBY STARS

Star	E	h	$\tilde{\omega}_{min}$	$\tilde{\omega}_{max}$	z_{min}	z_{max}	e
	(100 km^2 s^{-2})	(10 km kpc s^{-1})	(kpc)		(kpc)		
GL1	−1320.53	112.03	3.51	9.15	− 0.41	0.41	0.45
GL166	−1134.51	186.59	6.33	12.55	− 0.61	0.61	0.33
GL191	−1403.80	− 48.54	1.17	8.58	− 1.02	1.01	0.76
GL411	−1238.39	151.41	5.70	9.32	− 1.39	1.39	0.24
GL445	−1230.98	145.47	5.14	9.98	− 1.61	1.61	0.32
GL699	−1068.59	200.99	6.33	15.32	− 0.44	0.46	0.42
GL820	−1244.26	150.86	5.16	9.93	− 0.03	0.03	0.32
GL845	−1224.97	163.98	5.94	9.83	− 0.12	0.12	0.25
GL887	−1145.07	183.84	6.47	11.93	− 1.06	1.06	0.30
GL905	−1307.70	130.52	4.45	8.81	− 0.08	0.08	0.33
LDS519A	− 315.95	−288.65	5.76	121.50	−20.29	20.69	0.91
LDS519B	− 289.38	−290.10	5.71	132.77	−20.86	20.89	0.92

IV. CONCLUSIONS AND SUMMARY

A very simple model for the mass distribution f the galaxy has been presented. The model is hown to represent well the rotation curve and the erpendicular force of the galaxy. The galactic otation constants derived from the model agree ith recent observational data.

As an illustration, the galactic orbits of a group of 2 nearby high velocity stars were numerically inte- rated. The speed with which the integrations were arried out, as well as the high accuracy of the con- ervation of the total energy and angular momen- um, show that the mass model indeed allows ef- cient and accurate numerical orbit computations. he similarity of the orbits to those obtained with ur previous model shows that the computed orbits re not very sensitive to the details of the adopted ass model.

We would like to express our gratitude to L. guilar, A. Poveda, J. Cantó and J. Espresate for seful discussions, and to an anonymous referee for is valuable comments and suggestions.

REFERENCES

arseth, S.J. 1966, Nature, 212, 57
llen, C. 1990, RevMexAA, 20, 67
llen, C., & Martos, M. A. 1986, RevMexAA, 13, 137. (Paper 1)
Allen, C., Martos, M. A., & Poveda, A. 1987, RevMexAA, 14, 213. (Paper 2)
Allen, C., & Martos, M. A. 1988, RevMexAA, 16, 25
Allen, C., Schuster, W.J., & Poveda, A. 1991, A&A, in press
Bahcall, J.N. 1984, ApJ, 276, 169
Bahcall, J.N. 1991, ApJ, submitted
Carlberg, R.G., & Innanen, K.A. 1987, AJ, 94, 666
Caldwell, J.A.R., & Ostriker, J.P. 1981, ApJ, 251, 61
Carney, B.W., Latham, D.W., & Laird, J.B. 1988, AJ, 96, 560
Cudworth, K.M. 1990, AJ, 99, 590
Fich, M., Blitz, L., & Stark, A. A. 1989, ApJ, 342, 272
Haud, U. 1984, Ap&SS, 104, 337
Hanson, R.B. 1987, AJ, 94, 409
Kerr, F. J., & Lynden-Bell, D. 1986, MNRAS, 221, 1023
Kuijken, K., & Gilmore, G. 1989, MNRAS, 239, 605
Leonard, P.J.T., & Tremaine, S. 1990, ApJ, 353, 486
Martinet, L. 1974, A&A 32, 329
Miyamoto, M., & Nagai, R. 1975, Pub.Astr.Soc.Japan, 27, 533
Ollongren, A. 1962, BAN, 16, 241
Oort, J.H. 1960, BAN, 15, 45
Plummer, H.C. 1911, MNRAS, 71, 460
Roberts, M.S., & Whitehurst, R.W. 1975, AJ, 201, 327
Rubin, V.C., Ford, W.K., & Thonnard, N. 1980, ApJ, 238, 471
Rubin, V.C. 1983, in Kinematics, Dynamics and Structure of the Milky Way, Ed. W.L.H. Shuter (Dordrecht: D. Reidel), p.379
van de Kamp, P. 1971, ARA&A, 9, 103
Zaritsky, D., Olszewski, E.W., Schommer, R.A., Peterson, R.C., & Aaronson, M. 1989, ApJ, 345, 759

hristine Allen and Alfredo Santillán: Instituto de Astronomía, UNAM, Apartado Postal 70-264, 04510 México, D.F., México.

© Universidad Nacional Autónoma de México • Provided by the NASA Astrophysics Data System